Vacancy Cluster Evolution in Metals Under Irradiation

M.F. Wehner and W.G. Wolfer

August 1984
(revised January 1985)

UWFDM-590

FUSION TECHNOLOGY INSTITUTE

UNIVERSITY OF WISCONSIN

MADISON WISCONSIN

"LEGAL NOTICE"

"This work was prepared by the University of Wisconsin as an account of work sponsored by the Electric Power Research Institute, Inc. ("EPRI"). Neither EPRI, members of EPRI, the University of Wisconsin, nor any person acting on behalf of either:

"a. Makes any warranty or representation, express or implied, with respect to the accuracy, completeness, or usefulness of the information contained in this report, or that the use of any information, apparatus, method, or process disclosed in this report may not infringe privately owned rights; or

"b. Assumes any liabilities with respect to the use of, or for damages resulting from the use of, any information, apparatus, method or process disclosed in this report."

Vacancy Cluster Evolution in Metals Under Irradiation

M.F. Wehner and W.G. Wolfer

Fusion Technology Institute
University of Wisconsin
1500 Engineering Drive
Madison, WI 53706

http://fti.neep.wisc.edu

August 1984 (revised January 1985)

UWFDM-590

VACANCY CLUSTER EVOLUTION IN METALS UNDER IRRADIATION

M.F. Wehner

W.G. Wolfer

Fusion Engineering Program
Nuclear Engineering Department
University of Wisconsin-Madison
Madison, Wisconsin 53706

August 1984
Revised January 1985

UWFDM-590

VACANCY CLUSTER EVOLUTION IN METALS UNDER IRRADIATION

M.F. Wehner* and W.G. Wolfer

Fusion Engineering Program, Department of Nuclear Engineering
University of Wisconsin-Madison, Madison, Wisconsin 53706, USA

ABSTRACT

A stochastic treatment of vacancy cluster formation in irradiated metals is formulated in terms of a Fokker-Planck equation. The Fokker-Planck coefficients are found to depend on the cluster size distribution itself. This nonlinear equation is solved by a previously developed numerical path integral solution. The nonlinear dependence provides an important feedback for the evolution of the bias. This evolution both initiates and terminates the nucleation process. The void size distribution follows a bifurcation process in which a peaked distribution of stable voids separates from a distribution of small unstable voids. The stable void number density reaches a final value which depends on temperature and dose rate. These predicted values are in close agreement with measured void number densities.

---

*Present Address: Lawrence Livermore National Laboratory, Livermore, CA 94550, USA

1. INTRODUCTION

The formation of vacancy clusters and voids in solids subject to displacement damage has in the past been treated in the context of classical nucleation theory (Katz and Wiedersich, 1971; Russell, 1971, 1978; Wolfer and Si-Ahmed, 1982). The basic assumptions of the classical theory are that an incubation period or a lag time exist during which a subcritical cluster population forms. This period is then followed by a nucleation period during which a constant flux of clusters grows beyond a critical size. An individual cluster overcomes the nucleation barrier at the critical size only as a result of growth fluctuations. Once it crosses the barrier its further growth becomes more deterministic and growth fluctuations become negligible. The second important assumption of the classical and homogeneous nucleation theory concerns the termination of the nucleation period and the cessation of the steady-state nucleation rate. This termination is generally believed to be caused by a depression of the supersaturation of the clustering species, namely the concentrations of vacancies, divacancies and self-interstitials in the present example. For a continuous irradiation, the increasing void density is believed to eventually reduce the vacancy supersaturation and thereby stop the cluster flux across the nucleation barrier. Although it is difficult to precisely specify the required reduction, Russell (1978) suggests that a lowering of the vacancy supersaturation by a factor of ten will suffice to terminate void nucleation.

In this classical approach to void nucleation, the critical size and the nucleation barrier are determined mainly by the supersaturations, the internal energy of the cluster, and by the diffusion coefficients of the mobile

species. The subcritical cluster population below the critical size has no direct influence on the critical size and the nucleation barrier.

It is one of the major goals of the present paper to show that this latter assumption is incorrect. To abandon it requires also to abandon the classical approach of steady-state nucleation, and to develop a time-dependent theory which describes the evolution of the entire cluster population. This population is represented by a distribution function $P(x,t)$, where t is the time and x the number of vacancies contained in a cluster. For each cluster size x, the master equation determines the change of $P(x,t)$. The most direct approach to a time-dependent nucleation theory is then to numerically solve a sufficiently large group of master equations (Courtney, 1962; Abraham, 1969, 1971). An approximate numerical solution of the master equation has been developed by Kiritani (1973) by combining several individual rate equations into groups. Another approach is based on the Monte Carlo method, as has been used extensively by Binder (1984).

The first approach does not seem to be practical in view of the fact that voids observed in the electron microscope range in size from about 2 nm to 200 nm in diameter, and the barely visible voids already contain 300 vacancies. The second approach does not allow the void size distribution present at any moment to influence the subsequent evolution of the void population.

Accordingly, a different approach has been developed which proceeds along the following lines. In the first step, the master equation for the cluster distribution function $P(x,t)$ is replaced by a Fokker-Planck equation in the cluster size space x. Next, a nonlinear transformation between x and the cluster radius r is applied, and a new Fokker-Planck equation is obtained for the cluster distribution function $\tilde{P}(r,t)$. This Fokker-Planck equation is then

solved numerically using a recently developed technique based on the path integral (Wehner and Wolfer, 1983a, 1983b). These steps are discussed in Sections 2 and 3.

The reaction rates for the absorption and emission of mobile point defects at vacancy clusters depend most critically on three parameters, namely the so-called bias factors, the point defect concentrations, and the cluster properties. To make the paper self-contained, these parameters will be briefly summarized and discussed in Section 4. The results for the evolution of the vacancy cluster size distribution will then be presented in Section 5, and critically examined in Section 6.

2. MASTER AND FOKKER-PLANCK EQUATIONS

Let x denote the number of vacancies contained in a cluster and P(x,t) the number density of clusters of size x at time t. If it is assumed that a cluster of size x can change its size only by the absorption of monovacancies and of self-interstitials, and by the emission of vacancies, then the following master equation holds:

$$dP(x,t)/dt = \beta(x-1)P(x-1,t) + [\alpha(x+1) + \theta(x+1)]P(x+1,t) - [\alpha(x) + \beta(x) + \theta(x)]P(x,t) \quad (1)$$

This equation is valid for $x \geq 2$, and it represents a set of rate equations as x is a discrete variable assuming only integer values. The rate coefficients $\alpha(x)$, $\beta(x)$, and $\theta(x)$ are the absorption rates for vacancies and interstitials, and the thermally induced emission rate of vacancies from a cluster of size x, respectively. The thermally induced emission rate of interstitials is so

small as to be entirely negligible. Although the two absorption rates are strictly functions of time through their dependence on the point defect concentrations, this dependence can be suppressed for the following reason. The point defect concentrations, C_v and C_i for vacancies and interstitials, depend on the radiation induced production rate, P_o, and on the total sink strength S, a parameter that will be defined later. For a constant production rate P_o, the time dependence of S determines the time dependence of the concentrations C_v and C_i. These concentrations adjust to a new sink strength with a relaxation time on the order of S/D_v or less, where D_v is the diffusion coefficient for vacancy migration. Since this relaxation time is very short compared to the time scale over which S and P(x,t) change, we can indeed assume that the point defect concentrations are quasi-stationary, and $\alpha(x)$ and $\beta(x)$ are nearly time-independent. The expressions for the rate coefficients that will be used later are derived from a diffusion model of point defects to a spherical cavity. Accordingly, the size variable, x, in this model is treated as a continuous variable, and we shall therefore treat it likewise in the distribution function P(x,t).

For clusters with size $x >> 1$, we may expand the first and second term into Taylor series. Retaining terms only to second order, the master equation (1) is then approximated by the Fokker-Planck equation

$$\frac{\partial P(x,t)}{\partial t} = - \frac{\partial}{\partial x} [K(x)P(x,t)] + \frac{1}{2} \frac{\partial^2}{\partial x^2} [Q(x,t)P(x,t)] \qquad (2)$$

with a drift force defined as

$$K(x) = \beta(x) - \alpha(x) - \theta(x) \qquad (3)$$

and a diffusion function as

$$Q(x) = \alpha(x) + \beta(x) + \theta(x) \ . \tag{4}$$

This approximation to the master equation, originally due to Kramers (1940) and Moyal (1949) is valid only if the higher order terms are sufficiently small that they may be ignored. A truncation after the second term is particularly desirable as a theorem by Pawula (1967) assures that the distribution function $P(x,t)$ remains everywhere positive in this case. The smallness of the higher order terms in the expansion has been of great concern in the literature. Van Kampen (1961, 1981) has developed the so-called system size expansion as a systematic procedure to eliminate these terms. The necessary mathematical rigor was provided later by Kurtz (1971). Because of the unit step size, in the region $x >> 1$ the expansion and truncation is equivalent to such a procedure. Significant differences between the solutions to the master and to the Fokker-Planck equation would be expected in the vicinity of $x = 1$. However, we now introduce the boundary condition

$$P(1,t) = C_V \text{ for } t > 0 \ , \tag{5}$$

and thereby force the solution of the Fokker-Planck equation to agree with the solution to the master equation at $x = 1$. As a result we expect that the Fokker-Planck equation will provide adequate results for the entire size space $x \geq 1$. Additional boundary conditions are

$$P(x,0) = 0 \text{ for } x > 1 \tag{6}$$

and $$P(\infty,t) = 0 \ . \tag{7}$$

The solution for the cluster distribution in terms of the size variable x is not convenient for two reasons. First, for large voids such as those observed in irradiated materials, x becomes on the order of 10^6. Second, void size distributions are measured in terms of the void radius. Therefore, it is desirable to introduce a new cluster distribution function

$$\tilde{P}(r,t) = P(x,t) \frac{dx}{dr} \tag{8}$$

where the cluster or void radius is defined as

$$r = \left(\frac{3\Omega x}{4\pi}\right)^{1/3} + \frac{b}{2} \ . \tag{9}$$

Here, Ω is the atomic volume, and the cluster or void surface is defined by the centers of the surface atoms. Their radii is assumed to be equal to half the Burger's vector b. The equation (9) represents a nonlinear transformation between two stochastic variables, x and r. Using Eqs. (8) and (9) to transform the Fokker-Planck equation (2) and rearranging the terms to have the same form yields

$$\frac{\partial \tilde{P}}{\partial t} = \frac{\partial \tilde{P}(r,t)}{\partial t} = - \frac{\partial}{\partial r} \left[\tilde{K}(r)\tilde{P}(r,t)\right] + \frac{1}{2} \frac{\partial^2}{\partial r^2} \left[\tilde{Q}(r)\tilde{P}(r,t)\right] \tag{10}$$

where $$\tilde{K}(r) = K[x(r)] \frac{dr}{dx} + \frac{1}{2} Q[x(r)] \frac{d^2r}{dx^2} \tag{11}$$

$$\cong K(r) \frac{\Omega}{4\pi r^2} - Q(r) \frac{\Omega^2}{(4\pi)^2 r^5} \tag{12}$$

and $$\tilde{Q}(r) = Q[x(r)]\left(\frac{dr}{dx}\right)^2 \cong Q(r)\,\frac{\Omega^2}{(4\pi)^2 r^4}\,. \qquad (13)$$

One might also consider Eq. (2) as being equivalently described by a stochastic differential equation of the Ito type (Gardiner, 1983). The transformed coefficients can then also be obtained from the associated stochastic calculus. It will be shown below that the rate coefficients are all proportional to r. Hence, K(x) and Q(x) are both proportional to $x^{1/3}$, and the shift and diffusional broadening appear of equal importance. In contrast, the transformed drift force behaves as $\tilde{K}(r) \sim 1/r$ and the transformed diffusion function as $\tilde{Q}(r) \sim 1/r^3$. Therefore, with larger void radius, the diffusional spreading of the size distribution diminishes and void growth becomes an increasingly deterministic process when judged by the evolution of the void radius. The dynamics of void nucleation and growth are, of course, independent of the coordinate system used. The nonlinear transformation (9) simply illustrates that large voids are subject to smaller fluctuations in size than are small voids. The experimental evidence for this observation will be discussed in Section 6.

3. PATH SUM SOLUTION

The formal solution to the Fokker-Planck equation (10) subject to the boundary conditions of Eqs. (5) and (7) can be constructed via the path sum as shown recently by Wehner and Wolfer (1983b). If the solution at time t is assumed to be known, the solution at a later time $t + \tau$ is given by

$$\tilde{P}(r,t+\tau) = \int_b^\infty dr'\ \tilde{P}(r',t)G(r,r',\tau) - \int_o^\tau d\tau' \left[\tilde{J}(b,t+\tau')G(r,b,\tau') + \frac{1}{2}\tilde{P}(b,t+\tau')\tilde{Q}(b)\frac{\partial}{\partial r'}G(r,r'=b,\tau')\right] . \tag{14}$$

Here,

$$\tilde{J}(r,t) = \tilde{K}(r)\tilde{P}(r,t) - \frac{1}{2}\frac{\partial}{\partial r}\left[\tilde{Q}(r)\tilde{P}(r,t)\right] \tag{15}$$

is the net cluster current, and the radius of a monovacancy ($x = 1$) is assumed to be approximately equal to the Burgers vector b. In actual fact, the transformation (9) yields $r = 1.053\ b$ for $x = 1$ for the parameters of Table I.

In the limit of small time steps τ, the propagator or Green's function can be given by (Dekker, 1976)

$$G(r,r',\tau) = (2\pi\tilde{Q}(r')\tau)^{-1/2} \exp\{-[r - r' - \tilde{K}(r')\tau]^2/2\tilde{Q}(r')\tau]\} . \tag{16}$$

By the repeated application of Eq. (14) for N times, the solution can be found for a finite time interval $t - t_o = N\tau$. This solution becomes exact in the limit $\tau \to 0$ and $N \to \infty$ such that $N\tau$ remains fixed. In actual numerical calculations, a small but finite time step τ is selected based on the interval spacing employed in the numerical integration of Eq. (14). Furthermore, if τ is sufficiently small, $\tilde{P}(r,t)$ changes little in the vicinity of $r > b$, hence the cluster current $\tilde{J}(b,t+\tau')$ may be approximated by its value at time t. As a result of the boundary condition in Eq. (5), $\tilde{P}(b,t+\tau') = C_v$. Hence, the r.h.s. of Eq. (14) is known and can be evaluated.* The details of the numerical procedure are given elsewhere (Wehner and Wolfer, 1983b). Starting with

the initial condition, Eq. (6), the path sum solution of Eq. (14) then yields the evolution of the distribution function $\tilde{P}(r,t)$ with time.

4. RATE COEFFICIENTS, BIAS FACTORS AND POINT DEFECT CONCENTRATIONS

The fundamental process involved in the cluster formation is the diffusion of the point defects to the sinks. If we consider then a cluster as a spherical sink, and if the point defect absorption and emission at the sink is controlled by bulk diffusion, then the reaction rates are given by

$$\alpha(r) = 4\pi r D_i C_i Z_i^o(r) \tag{17}$$

$$\beta(r) = 4\pi r D_v C_v Z_v^o(r) \tag{18}$$

$$\theta(r) = 4\pi r D_v C_v^o(r) Z_v^o(r) \tag{19}$$

where
$$C_v^o(r) = C_v^{eq} \exp\{4\pi[\gamma(r)r^2 - \gamma(r_-)r_-^2]/kT\} \tag{20}$$

is the vacancy concentration in local thermodynamic equilibrium with a void of radius r, $\gamma(r)$ is the surface energy, and r_- is the radius of the void with one less vacancy. The surface energy for small voids is dependent on the void radius as discussed by Si-Ahmed and Wolfer (1982).

The void bias factors $Z_i^o(r)$ and $Z_v^o(r)$ account for the effect of the stress-induced interaction of the interstitial and vacancy, respectively, with

*Note that since Eq. (13) is a parabolic partial differential equation, both the value of the probability distribution and the current may not be specified independently at the boundary without a risk of overspecifying the problem (Morse and Feshbach, 1953).

the void. They have been derived recently by Sniegowski and Wolfer (1983) for the case where segregation to voids does not occur. Both bias factors are given by

$$Z^o(r) \cong 1 + [(\sqrt{1 + \eta} - 1)/2\lambda]^{1/3} \tag{21}$$

where

$$\eta = 4\lambda\Gamma/(r^3 kT \ln 2) \tag{22}$$

$$\Gamma = \frac{\mu v^2 (1 + \nu)^2}{36\ \pi(1 - \nu)} \tag{23}$$

$$\lambda = \frac{7 - 5\nu}{30} - \frac{2\Gamma\mu^2}{3r\alpha^G\gamma^2}\ . \tag{24}$$

Here, μ is the shear modulus, ν the Poisson's ratio, k the Boltzmann constant, and T the absolute temperature. By inserting the appropriate values for the relaxation volume v and the shear polarizability α^G, the bias factors Z_i^o and Z_v^o can be obtained for the absorption of self-interstitials and vacancies, respectively. For the materials parameters of solution-annealed nickel, listed in Table I, the void bias factors as shown in Fig. 1 are obtained. It is seen that small voids possess a significant bias for preferential interstitial absorption. However, this bias diminishes rapidly with increasing void radius, a fact that will prove to be essential for the emergence of a peaked distribution for voids above the critical size.

As mentioned in Section 2, the time scale for the relaxation of the point defect concentrations is much shorter than for significant change in the cluster population. Thus the point defect concentrations assume their stationary solutions corresponding to the existing set of material parameters,

Table I. Materials Parameters for Nickel

k	Boltzmann constant	1.38×10^{-23} J/°K
T	temperature	
a	lattice parameter	3.639×10^{-10} meter
b	Burger's vector	$a/\sqrt{2}$
Ω	atomic volume	$a^3/4$
E_v^m	vacancy migration energy	1.76×10^{-19} Joule
E_v^f	vacancy formation energy	2.832×10^{-19} Joule
D_v	vacancy diffusion coefficient	$1.286 \times 10^{-6}\, e^{-E_v^m/kT}$ (m^2/s)
P_o	production rate of point defects	$0.1\ \Omega$ x (dpa rate)
R_c	recombination coefficient	$8\pi a\left(\frac{1}{D_i} + \frac{1}{D_v}\right) \sim \frac{8\pi a}{D_v}$
C_v^{eq}	equilibrium vacancy concentration	$\frac{1}{\Omega} e^{(1.5-E_v^f/kT)}$ (m^{-3})
ν	Poisson's ratio	$0.264 + 7.7 \times 10^{-5}$ T (°C)
E	Young's modulus	$2.097 \times 10^{11} - 1.03 \times 10^{8}$ T (°C) (pascals)
μ	shear modulus	$E/2(1 + \nu)$
v	relaxation volume	for interstitials $1.8\ \Omega$
		for vacancies $-0.2\ \Omega$
α^G	shear polarizability	for interstitials -150 eV
		for vacancies -15 eV
γ_o	surface energy of flat surface	$2.28 + (1333 - T)0.55 \times 10^{-3}$ J/m^2
$\gamma(x)$	surface energy of a void	$\gamma_o[1.0 - (0.8/(x + 2))]$
A^d	shape factor for dislocations	
ρ^d	dislocation density	
$A^d\rho^d$	dislocation sink strength	2×10^{13}
$Z^d_{i,v}$	dislocation bias factors	

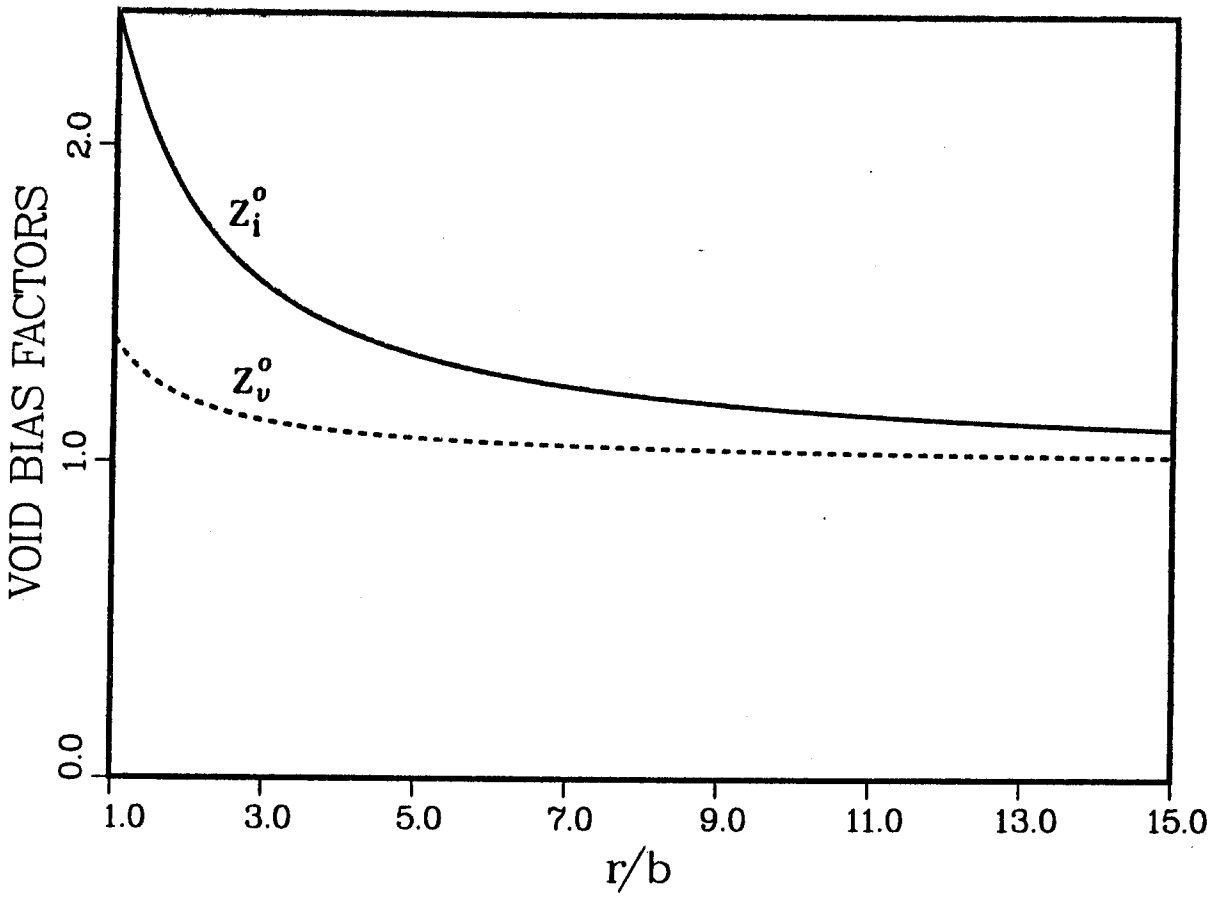

Figure 1. The void bias factors vs. void radii for interstitials (solid line) and for vacancies (dashed lines) evaluated from Eqs. (18) and with the parameters listed in Table I.

and C_i and C_v change as these parameters change. The approximation $dC_i/dt \cong dC_v/dt \cong 0$ is a statement of the "adiabatic approximation" as termed by Haken (1983). The resulting equations for the point defect concentrations become (Si-Ahmed and Wolfer, 1982)

$$D_i C_i = \frac{1}{2}\left\{\left[\left(\frac{\langle Z_v\rangle}{\langle Z_i\rangle} D_v C_v^s + \frac{S\langle Z_v\rangle}{R_c}\right)^2 + \frac{4\langle Z_i\rangle}{\langle Z_v\rangle R_c} P_o\right]^{1/2} - \left(\frac{\langle Z_v\rangle}{\langle Z_i\rangle} D_v C_v^s + \frac{S\langle Z_v\rangle}{R_c}\right)\right\} \tag{25}$$

and

$$D_v C_v = \frac{\langle Z_i\rangle}{\langle Z_v\rangle} D_i C_i + D_v C_v^s .$$

Here the total sink strength is

$$S = 4\pi \int_b^\infty dr\, [r\tilde{P}(r,t)] + A^d \rho^d \tag{26}$$

the sink averaged bias factors are

$$\langle Z\rangle = \frac{4\pi \int_b^\infty dr\, [r Z^o(r)\tilde{P}(r,t)] + Z^d A^d \rho^d}{S} \tag{27}$$

and the averaged vacancy concentration in equilibrium with sinks is

$$C_v^s = \frac{4\pi \int_b^\infty dr\, [r C_v^o(r) Z_v^o(r)\tilde{P}(r,t)] + C_v^{eq} Z_v^d A^d \rho^d}{\langle Z_v\rangle} . \tag{28}$$

One may speak of the fast variables (the point defect concentrations) as being "slaved" by the slow variables (the average bias factors, the sink strength and the averaged vacancy concentration). Moreover, the dependence of the point defect concentrations on the cluster size distribution leads to another important consequence. Through Eqs. (17-19) and (25-28) one can see that this

dependency removes the linearity of the Fokker-Planck equation (13). Indeed Eq. (10) is no longer a differential equation but rather an integrodifferential equation. Such integral dependencies are common throughout physics whenever many-body interactions play an important role. In the present case, the integral dependence arises from the fact that the mono-defect populations depend on weighted averages of certain functions characteristic of the system. It does not, however, depend on particular values of the size distribution function. Because of this integral dependence, this truly nonlinear equation can be solved using the numerical path integral technique by assuming that for small enough time steps the equation may be regarded as being linear. Then given the solution at a particular time, the solution a very short time later can be found. This new solution is used to recalculate the point defect concentrations (and hence the Fokker-Planck coefficients). A revised linear equation is constructed and the whole process repeated. In this manner it is possible to investigate the effect of the void size distribution on its own development.

5. VOID SIZE DISTRIBUTIONS

In order to gain an initial understanding of the dynamics of void nucleation, the nonlinear character of Eq. (10) will be suppressed. Specifically, the integral dependence in Eqs. (26-28) will be neglected. This erroneous assumption leads to the conclusion that the microstructural properties of the material remain unchanged throughout the nucleation process. Nevertheless, certain interesting characteristics of cluster nucleation become transparent in this limit.

Figures 2a and 2b show the transformed Fokker-Planck coefficients evaluated for parameters listed in Table I and for a case representative of ion bombardment experiments at a temperature of 873 K. The total sink strength was chosen to be somewhat higher than the dislocation sink strength alone and is kept at a constant value. The general shape of these plots is typical of that found over the entire ranges of temperature and dose rate studied. The critical size of a void is defined as that size where $\tilde{K}(r)$ crosses zero. This corresponds to the location of the peak of the nucleation barrier. In Fig. 2a, this occurs at approximately r/b = 3.0. At this point in the discussion, it is convenient to introduce some nomenclature. Voids of less than the critical size are subject to a negative drift force, hence they are more likely to be driven back in size space across the boundary at r/b ≈ 1. Since a "particle" driven across a boundary in an open system is lost, these voids are referred to as "unstable." Some voids, driven by the random forces, will cross the critical size. These voids are then subject to a positive drift force and tend to grow in size. Hence, voids of a size greater than the critical size are termed "stable."

Figure 3a shows the void size distribution obtained by solving the linear equation (10) subject to the Fokker-Planck coefficients of Fig. 2. As is evident, a large concentration of small unstable voids (invisible to the electron microscope) develops quite rapidly. In addition, after a certain length of time, a uniform, plateau-like distribution of larger stable voids is established. The leading edge of this plateau continues to propagate in size space as time progresses.

The nucleation barrier for the linear Fokker-Planck equation is, of course, time-independent. Accordingly, the current across this barrier quick-

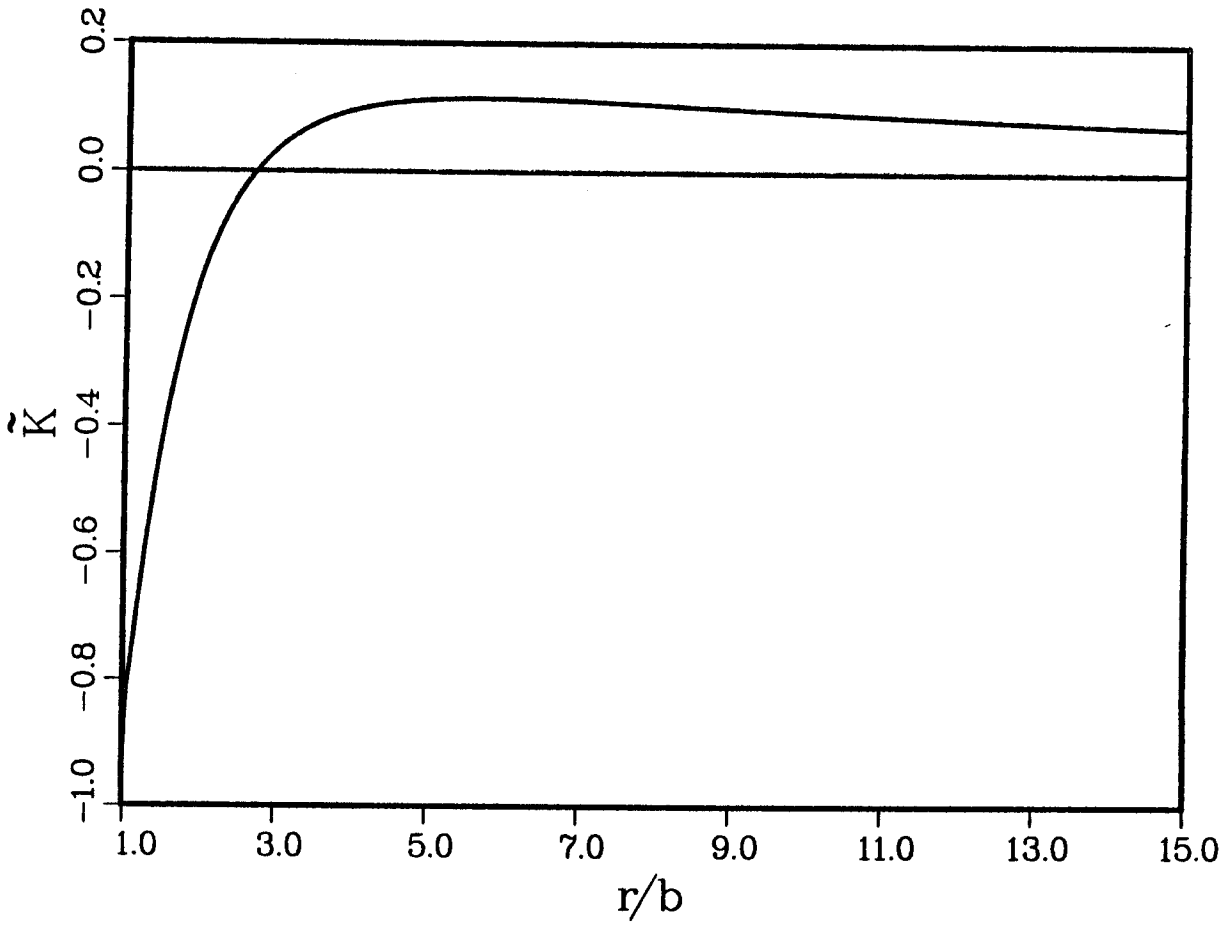

Figure 2a. The transformed drift function vs. void radii obtained by neglecting the effect of the void size distribution at T = 873 K and a dose rate of 0.001 dpa/s.

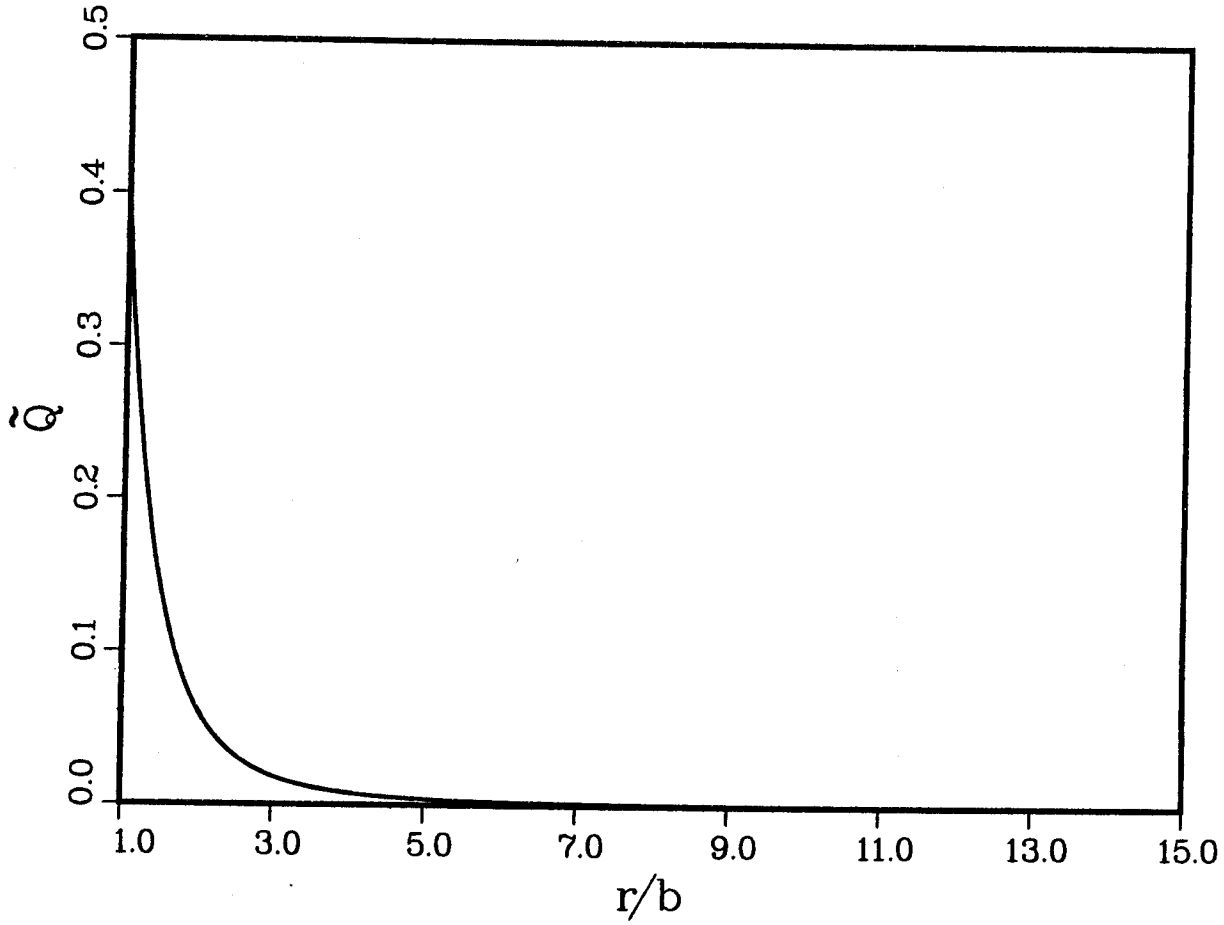

Figure 2b. The transformed diffusion function vs. void radii obtained by neglecting the effect of the void size distribution at T = 873 K and a dose rate of 0.001 dpa/s.

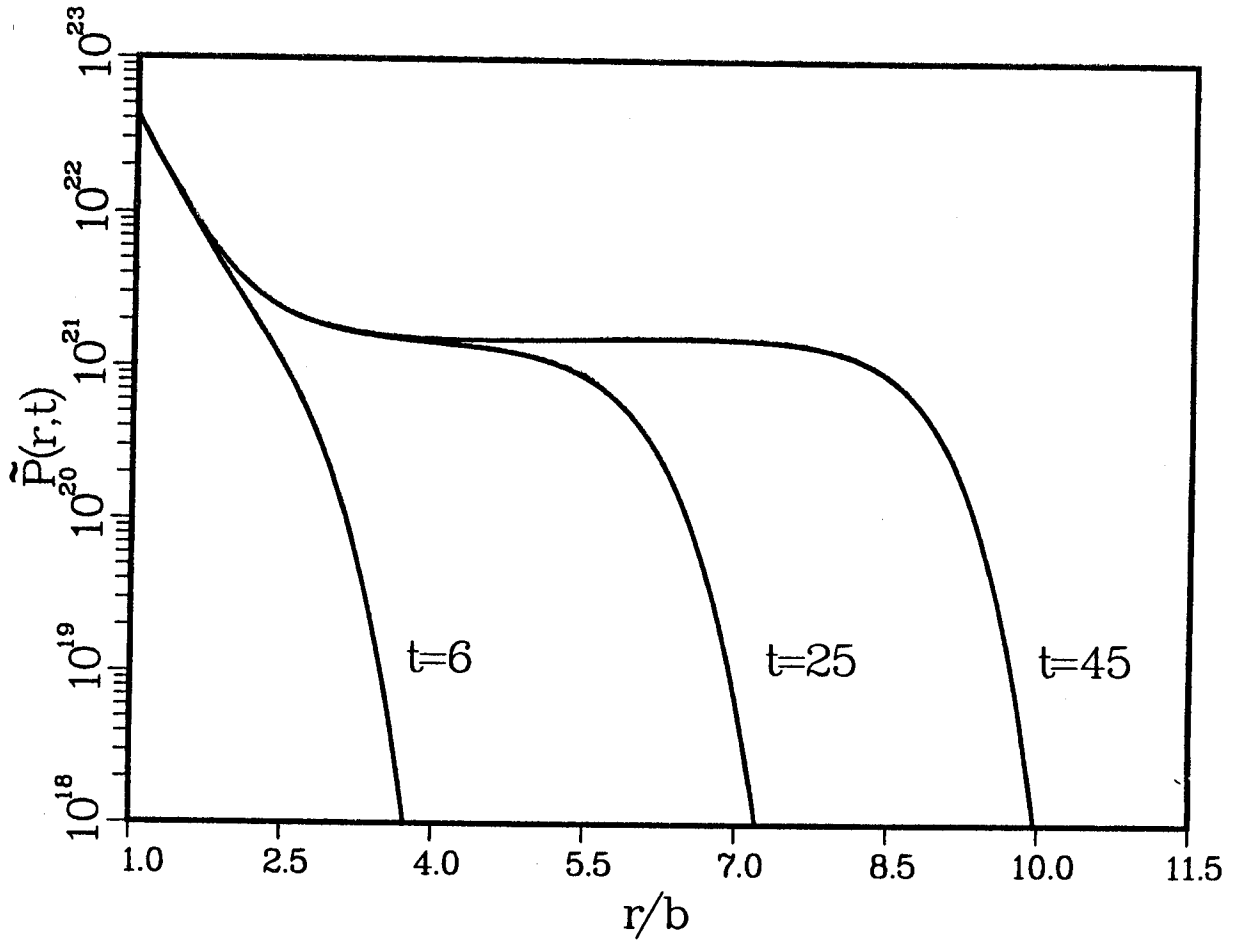

Figure 3a. The void size distribution vs. void radii at various times obtained by neglecting the effect of the size distribution upon itself at T = 873 K and a dose rate of 0.001 dpa/s. Note the high concentration of unstable voids and the plateau-like size distribution of stable voids. The times indicated are in seconds.

ly attains its steady-state value. This constant current, together with the slowly varying nature of the drift force of Fig. 2a in the region $r/b > 5$, causes the size distribution to flatten out. Hence, the plateau-like behavior is a consequence of the suppression of the nonlinearity of Eq. (10).

Computer memory limitations prohibit extension of the calculations to total doses much higher than 0.2 dpa for the Fokker-Planck coefficients plotted in Fig. 2. The trend, however, is that of a development of a population of voids uniformly distributed over a broad range in size. In addition, the void number density, defined as the area under the stable portion of the void size distribution, continues to increase with increasing dose. Both of these effects are contrary to experimental findings. Under most irradiation conditions, a very narrow size class of voids is observed, i.e. the void size distribution is sharply peaked. Also, the void number density does not vary with time after an initial nucleation period (Glasgow, Si-Ahmed, Wolfer, Garner, 1981; Mansur 1978). As Fig. 3a shows, this cannot be obtained by a theoretical approach which neglects the effect of the void population itself on the microstructural properties of the metal.

To this end, the nonlinear character of Eq. (10) is considered. Figure 3b shows the void size distribution at various times solved under the same conditions as in Fig. 3a except that the integrals of Eqs. (26-28) are calculated after each time step and the Fokker-Planck coefficients suitably adjusted as described in the previous section. These plots show a dramatic change in the void size distribution which now becomes very sharply peaked at the later times (note the logarithmic y axis). Also, the unstable voids diminish in number as time progresses. Furthermore, after the initial nucle-

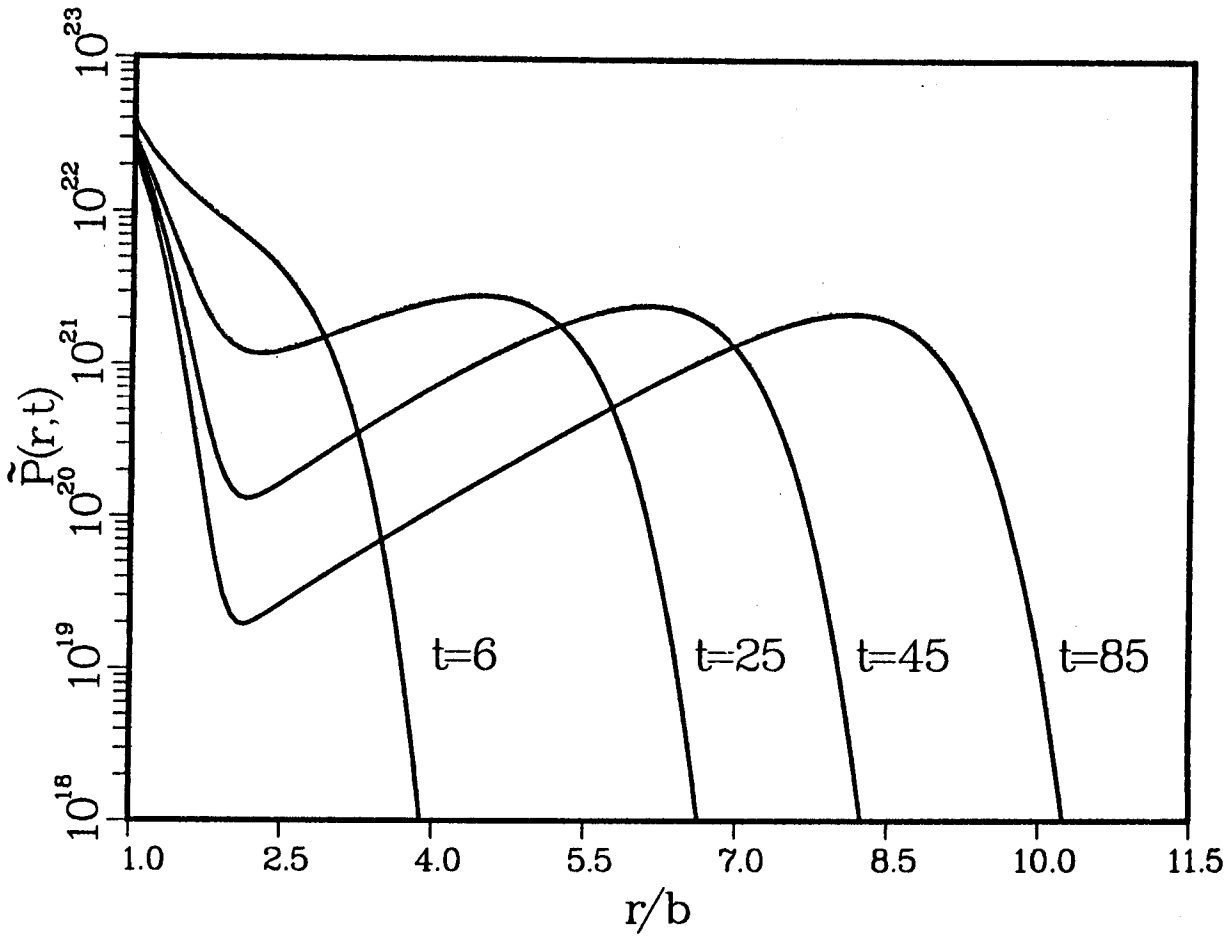

Figure 3b. The void size distribution vs. void radii at various times obtained by considering the effect of the void size distribution itself on the microstructural parameters at T = 873 K and a dose rate of 0.001 dpa/s. Note the "pinching off" of the void size distribution at later times. This results in a lowering of the concentration of unstable voids as well as the isolation of a narrow size class of stable voids. The times indicated are in seconds.

ation period, the stable void number density remains constant with increasing dose.

Such an extreme change in the shape of the distribution function illustrates the highly sensitive nature of void nucleation to changes in the microstructure and the rate coefficients. The feedback mechanisms responsible for the termination of void nucleation are twofold. First the increase in the void sink strength causes a decrease in the concentrations of both point defects. This feedback mechanism is however not as significant as traditionally believed. As seen from the y-intercepts in Fig. 3b, the vacancy concentration changes little with time.

The second, and dominant feedback mechanism is the change in the difference of the capture rates β and α. This difference is highly sensitive to changes in the average bias factors, and best illustrated by the transformed drift force $\tilde{K}(r)$. Figure 4 shows that the drift force not only changes in magnitude but the critical size increases as well with increasing dose. In terms of the number of vacancies contained in the void, x, the critical size is approximately 18, 56, 166, 460, for the various times indicated. The transformed diffusion function, $\tilde{Q}(r)$, being a sum rather than a difference of the rate coefficients, does not change much with time and has the general shape as in Fig. 2b. The changing shape of the distribution function can be further explained by defining a potential function as

$$G(r,t) = -2 \int_b^r \frac{\tilde{K}(r',t)}{\tilde{Q}(r',t)} dr' \quad . \tag{29}$$

The peak value of this potential determines the nucleation barrier, ΔG. As shown in Fig. 5, this barrier increases dramatically with time. Since the

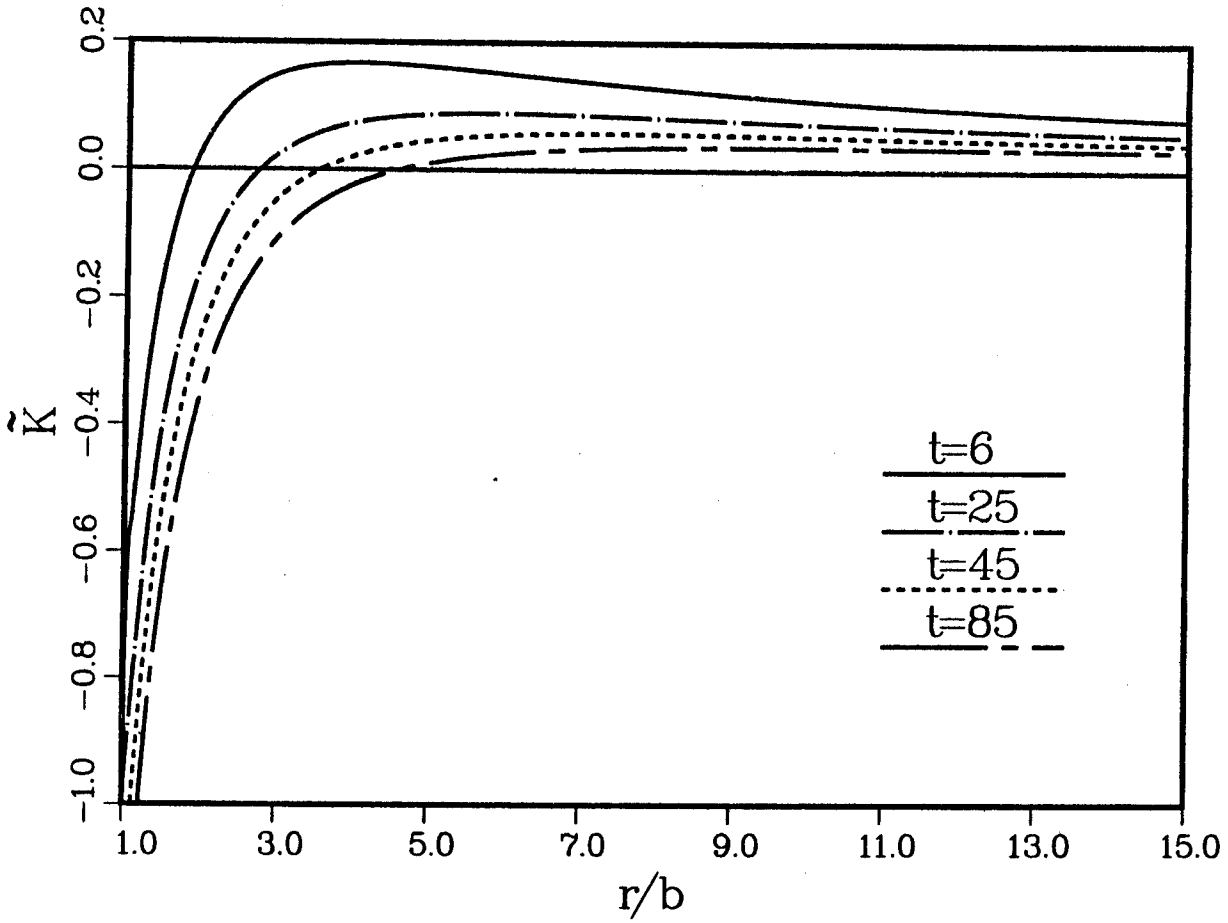

Figure 4. The transformed drift function vs. void radii which led to the void size distributions of Fig. 3b evaluated at those times.

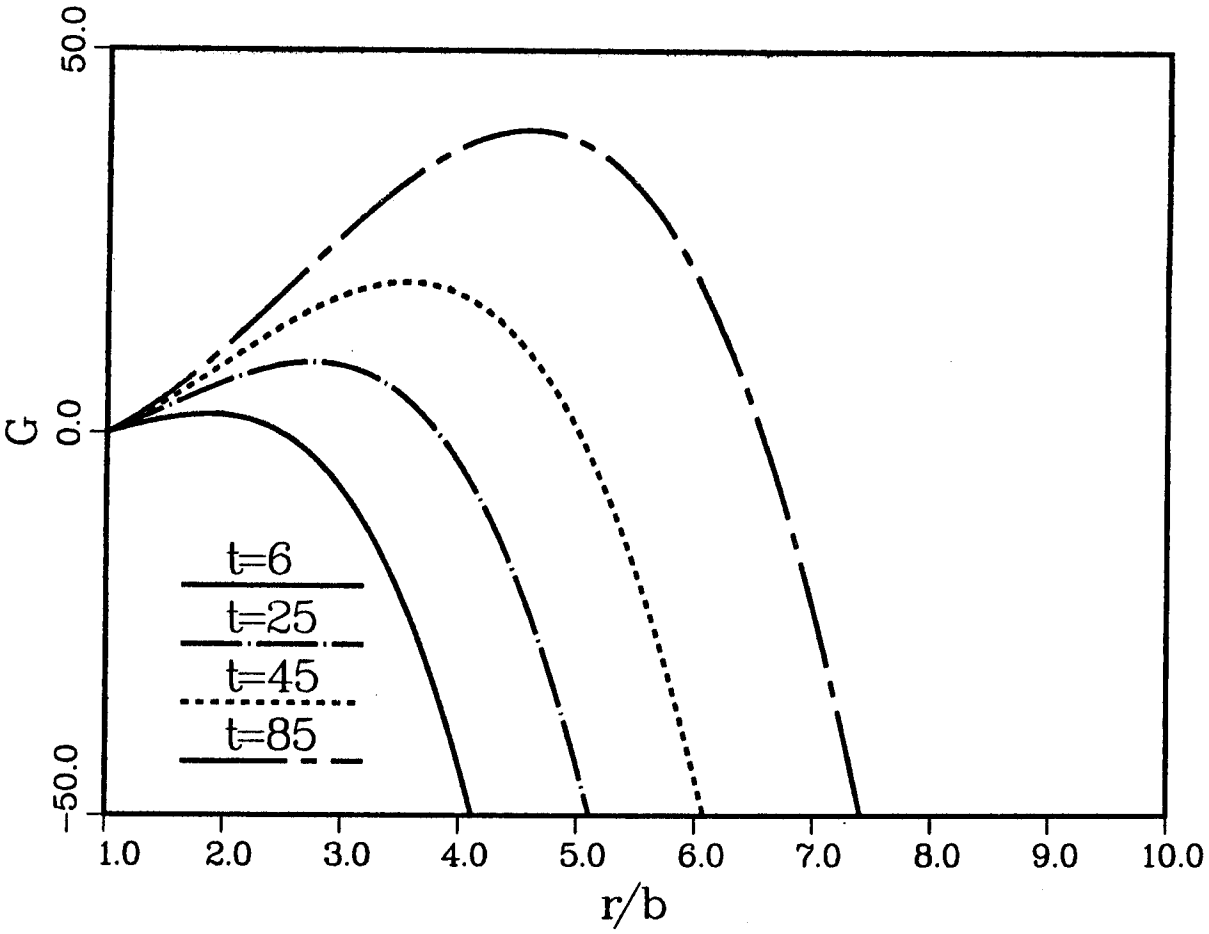

Figure 5. The potential function vs. void radii which led to the void size distributions of Fig. 3b evaluated at those times. Note how the nucleation barrier (the peak value of the potential) increases drastically with time.

steady state nucleation current over a fixed barrier is proportional to $e^{-\Delta G}$ (Russell, 1978), it is apparent that the time-dependent nucleation current corresponding to the barrier of Fig. 5 is reduced significantly in a very short period of time. Clearly, the actual nucleation of voids can occur only in the very early stages of the irradiation.

The irradiation temperature of the material determines to a large degree the point defect concentrations. Accordingly, the dynamics of void nucleation and growth are also expected to be strongly affected by the temperature. Figure 6a shows the calculated void size distribution obtained for ion bombardment of nickel at a temperature of 673 K. Comparison with the higher temperature (873 K) resultant of Fig. 3b, reveals two experimentally consistent observations. First, at the lower temperature, the stable void number density as well as the vacancy concentration are considerably higher. Second, the nucleation process requires more time (hence more total dose) at the lower temperature. However, the general shape of the void size distribution is the same in both figures.

The damage rate also affects the dynamics of void nucleation and growth by governing directly the point defect production. In Fig. 6b, the calculated void size distribution obtained for neutron bombarded nickel at a temperature of 673 K is shown. Comparison with the previous figure reveals a lower stable void number density, and that more time but less total damage is required for the nucleation process occurring at a lower damage rate.

Again the overall shape of the void size distribution, especially in the stable size regime, is the same. A comparison with several different combinations of temperature and dose rates confirms that the shape, more specifically the width at any fraction of the maximum of the stable void population

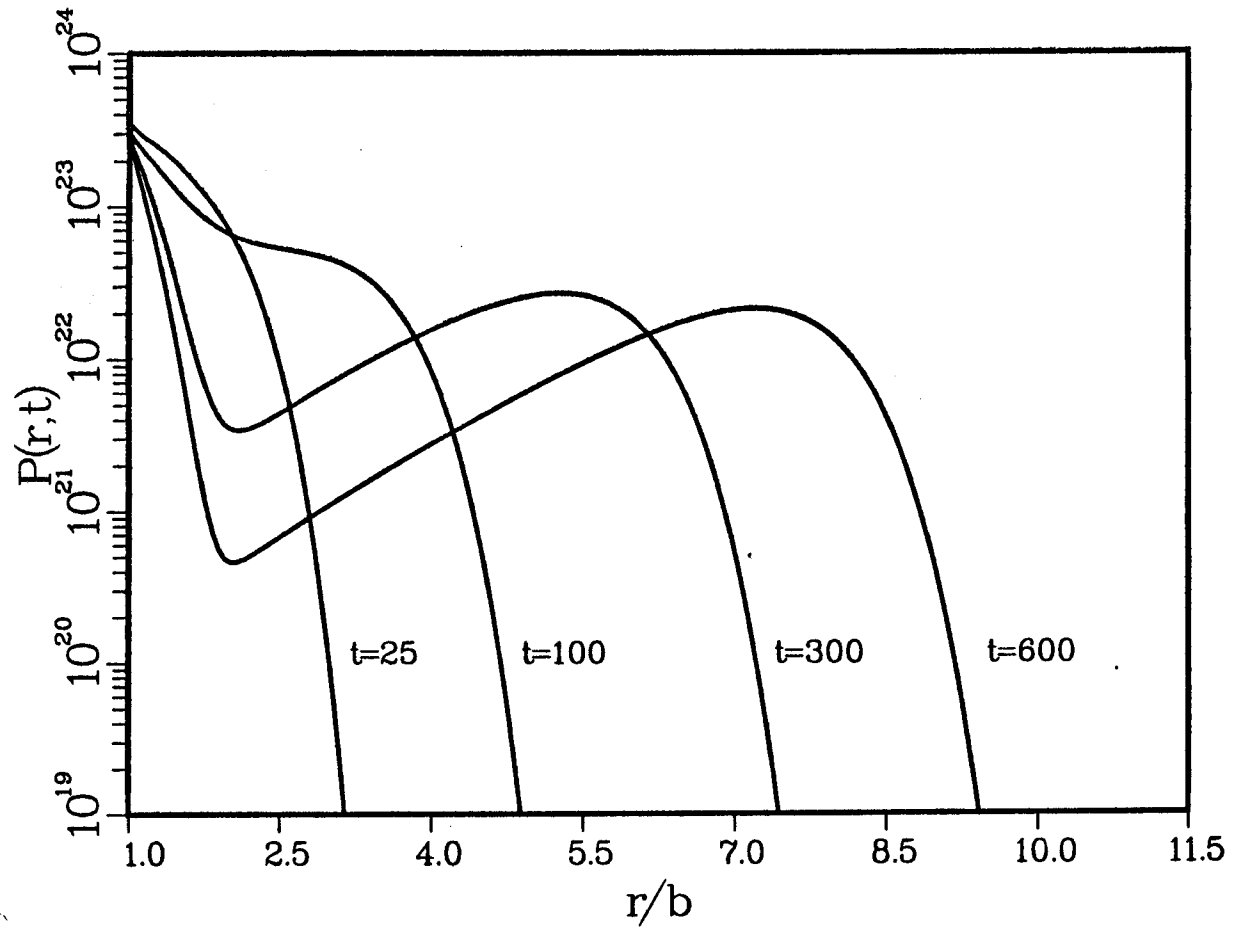

Figure 6a. The void size distribution vs. void radii at various times with T = 673 K and a dose rate of 0.001 dpa/s.

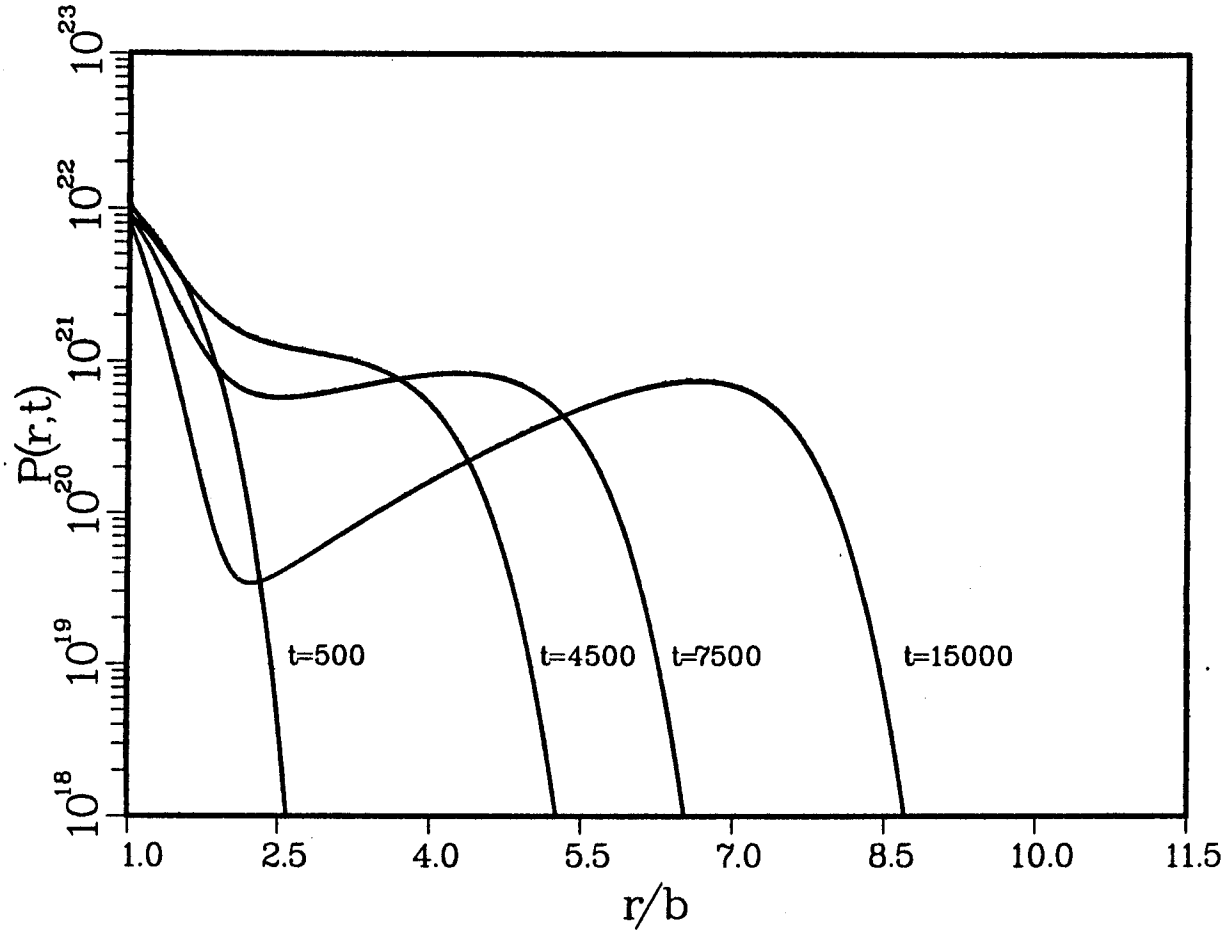

Figure 6b. The void size distribution vs. void radii at various times with T = 673 K and a dose rate of 10^{-6} dpa/s.

remains nearly constant over a wide range of values. In this study all other parameters characterizing the material were held constant. Other results not shown here indicate that the width of the size distribution broadens and the height diminishes as the dislocation sink strength increases significantly beyond the void sink strength. A more detailed analysis of the effect of this and other material parameters on void nucleation and growth is forthcoming.

6. DISCUSSION

The present results indicate that in annealed materials subject to displacement damage, the stable void size distribution is established at low doses. In contrast, most irradiation experiments are carried to higher doses because both measurements of void densities and void swelling can be performed with greater accuracy. These measurements are aimed at obtaining average void sizes and total number of voids per unit volume. Rarely are detailed void size distributions obtained. However, in the few cases where distributions have been measured with satisfactory statistical counts, the following characteristics are observed. The void size distribution at low doses is indeed sharply peaked in agreement with our results. However, a significant tail towards larger void sizes is often observed which is attributed to void coalescence. This process is not included in the present analysis based on the master equation (1) which allows only unit step processes. Extensive coalescence can furthermore lead to bi-modal void size distributions at high doses. Renucleation at higher doses due to helium production also gives rise to bi-modal void size distributions.

It should also be noted that many materials of practical interest such as steel are highly heterogeneous, and the spatial distribution of voids reflects this varying microstructure.

Accordingly, a comparison between our theoretical predictions and experimental results is best made on pure metals. Since the most commonly observed quantity is the void number density, the stable void size distribution was integrated from a void radius of 1 nm upwards. This lower bound represents the limit of visibility in standard transmission electron microscopy. Furthermore, the calculations of the void size distribution were always carried out to a sufficiently large dose to provide the terminal void number density. This density is plotted in Fig. 7 as a function of the irradiation temperature for various dose rates. It is seen that the void number density decreases sharply with temperature. With increasing dose rate, the characteristic curve for the total void number density is shifted to higher temperature. This shift is well known for the swelling-temperature relationships. When comparing heavy ion irradiations of a typical dose rate of 10^{-3} dpa with fast neutron irradiations ($\sim 10^{-6}$ dpa/s), we find a characteristic temperature shift for void nucleation of about 200°C in the case of nickel. This shift is somewhat larger than the corresponding shift for void growth (Brailsford and Bullough, 1972). Both the temperature and dose-rate dependence of the terminal void number density are in general agreement with the experimental observations. Furthermore, the quantitative comparison illustrated in Fig. 8 demonstrates that the predicted void number densities (solid line) are in excellent agreement with the measured void densities in nickel irradiated with fast neutrons at temperatures below about 500°C (Packan, Farrel and Stiegler, 1978; Brimhall and Mastel, 1968, 1969a, 1969b; Adda, 1971). The experimental

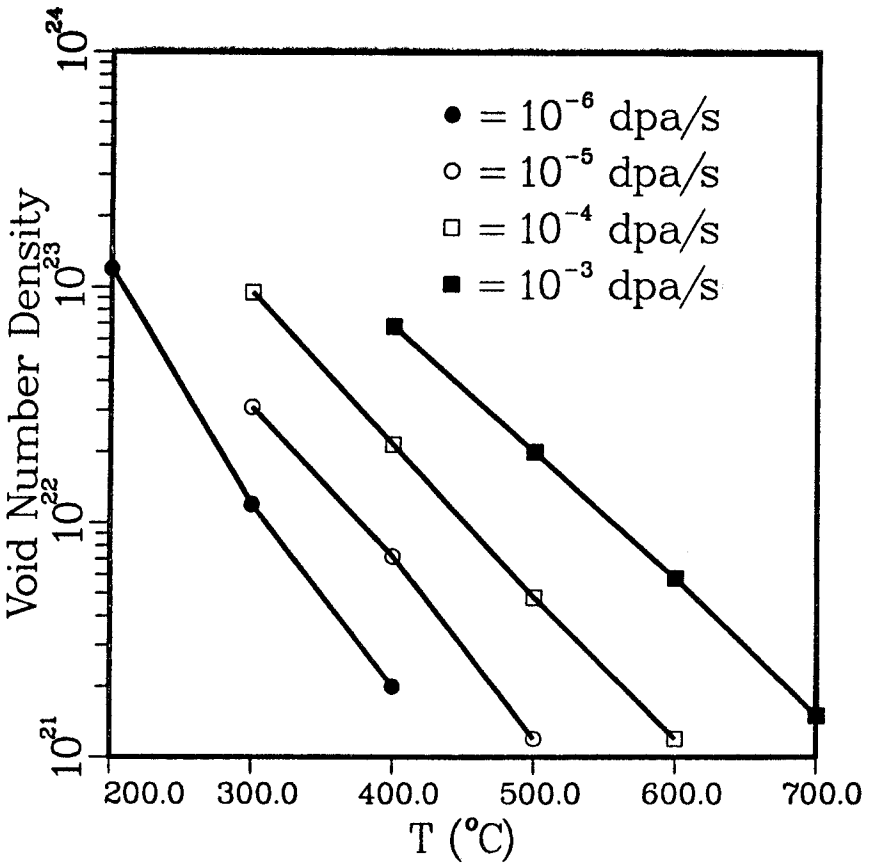

Figure 7. Terminal void number densities vs. temperature at various dose rates. Solid circles - 10^{-6} dpa/s; open circles - 10^{-5} dpa/s; open squares - 10^{-4} dpa/s; solid squares - 10^{-3} dpa/s.

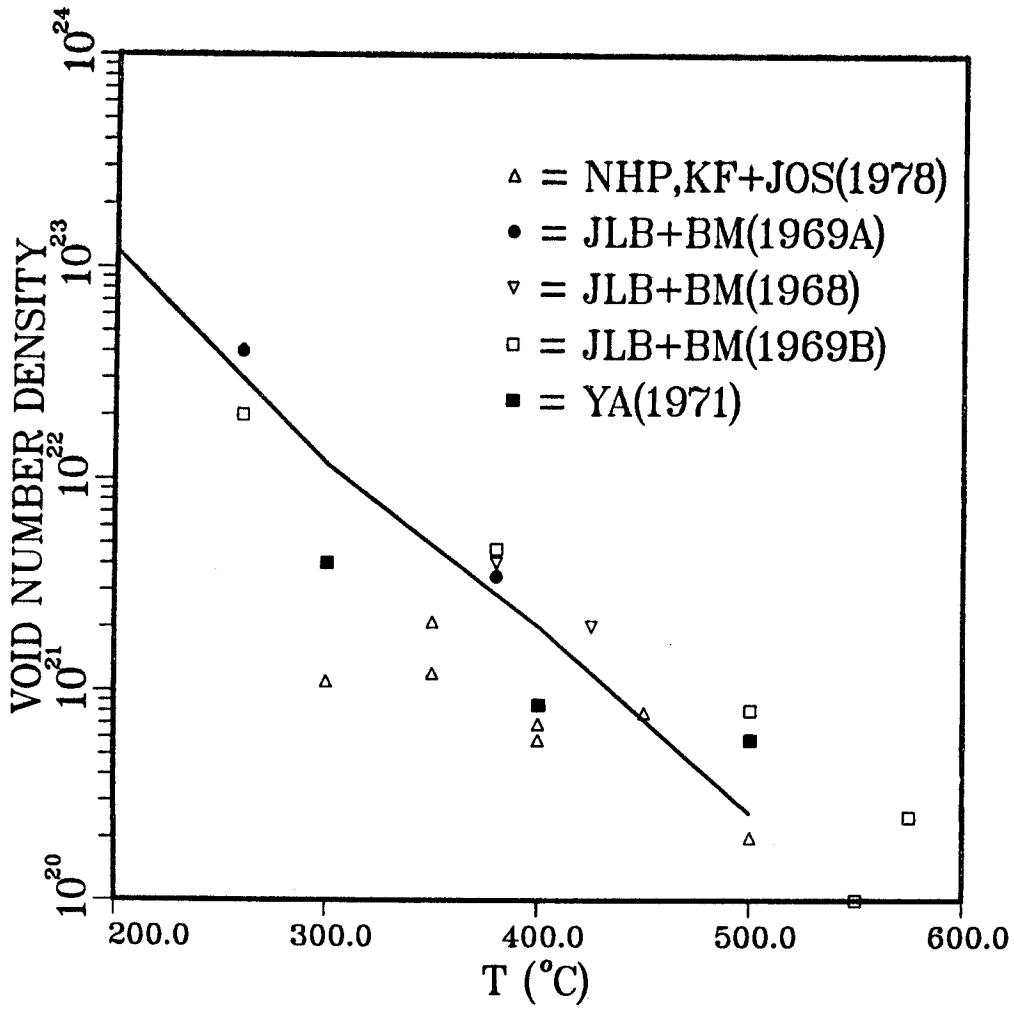

Figure 8. A comparison of the theoretical prediction of the terminal void number density vs. temperature with various neutron irradiation experiments.

data at higher irradiation temperatures reflect the presence of gas bubbles. Some of the data on void number densities reported by Packan, Farrel and Stiegler (1978) are for dose rates of 10^{-7} dpa/s, and therefore expected to fall below the solid curve predicted for a dose rate of 10^{-6} dpa/s.

The above comparison and agreement between measured and theoretically predicted void number densities is remarkable in several aspects. First, no parameter of the theoretical models required adjustment. The value of surface energy employed is the one measured for a clean surface of nickel; the bias is evaluated based on the elastic constants, the Burgers vector, and the actually measured relaxation volumes for interstitials and vacancies (Sniegowski and Wolfer, 1984). Second, no gas is required in the dynamic void nucleation calculations. The void nucleation is both self-starting and self-terminating. The autonomous process for void nucleation in an annealed metal reflects the importance of the feedback mechanisms discussed in the previous section. Among these, the evolution of the average bias provides the key for the emergence of a sharply peaked void size distribution. Such an evolutionary process can no longer be treated with the traditional theory of steady state nucleation. The approach developed in the present paper, based on the time dependent solution of a truly nonlinear Fokker-Planck equation, proved very successful in treating the dynamic nucleation process and the subsequent growth stage in a unified formalism.

The fact that no gas is required in the present dynamic void nucleation calculations is in apparent contradiction to the experimental observations by Norris (1970) who found no voids in pure annealed nickel irradiated in the high-voltage electron microscope. There are in fact other numerous experimental observations which clearly demonstrate the sensitivity of void nucle-

ation to small amounts of residual gases in the metal. To resolve this apparent inconsistency between theory and experiments we must conclude that the major role of gases is to prevent the collapse of vacancy clusters into dislocation loops, but is not responsible for their nucleation. This process, not incorporated into the present model, would be favored energetically when the cluster reaches a critical size (Sigler and Kuhlmann-Wilsdorf, 1966) and when it contains no gas.

ACKNOWLEDGEMENTS

The authors gratefully acknowledge the support by the Electric Power Research Institute under Contract No. RP1597-2 and by the National Science Foundation with the University of Wisconsin.

REFERENCES

Abraham, F.F., 1969, J. Chem. Phys. 51, 1632; 1971, ibid. 54, 3874.

Adda, Y., 1978, in "Radiation-Induced Voids in Metals," Corbett and Ianniello, eds., (CONF-710601), p. 31.

Binder, K., 1984, "Application of the Monte Carlo Method in Statistical Physics," (Berlin: Springer-Verlag).

Brailsford, A.D. and Bullough, R., 1972, J. Nucl. Mat. 44, 121.

Brimhall, J.L. and Mastel, B., 1968, J. Nucl. Mat. 28, 115.

Brimhall, J.L. and Mastel, B., 1969a, J. Nucl. Mat. 29, 123.

Brimhall, J.L. and Mastel, B., 1969b, J. Nucl. Mat. 33, 186.

Courtney, W.G., 1962, J. Chem. Phys. 36, 2009.

Gardiner, C.W., 1983, "Handbook of Stochastic Methods," (Berlin: Springer-Verlag) p. 96.

Glasgow, B.B., Si-Ahmed, A., Wolfer, W.G. and Garner, F.A., 1981, J. Nucl. Mat. 103 & 104, 981.

Haken, H., 1983, "Synergetics, An Introduction," 3rd ed., (Berlin: Springer-Verlag) p. 192.

Katz, J.L. and Wiedersich, H., 1971, J. Chem. Phys. 55, 1414.

Kiritani, M., 1973, J. Phys. Soc. Japan 35, 95.

Kramers, H.A., 1940, Physica 7, 284.

Kurtz, T.E., 1969, J. Chem. Phys. 50, 460.

Mansur, L.K., 1978, J. Nucl. Mat. 78, 156.

Morse, P.M. and Feshbach, H., 1953, "Methods of Theoretical Physics, Volume 1," (New York: McGraw-Hill) p. 705.

Moyal, J.E., 1949, J.R. Stat. Soc. 11, 151.

Norris, D.I.R., 1970, Nature 227, 830.

Packan, N.H., Farrel, K., and Stiegler, J.O., 1978, J. Nucl. Mat. 78, 143.

Pawula, R.F., (1967), Phys. Rev. 162, 186.

Russell, K.C., 1971, Acta Metall. 19, 753.

Russell, K.C., 1978, Acta Metall. 26, 1615.

Si-Ahmed, A. and Wolfer, W.G., 1982, Proceedings of the 11th International Symposium on the Effects of Radiation on Materials, ASTM STP 782 (Philadelphia: American Society for Testing Materials) p. 1008.

Sigler, J.A., and Kuhlmann-Wilsdorf, D., 1966, in "The Nature of Small Defect Clusters," M.J. Makin, Ed., Report AERE-R5269, Vo.. I, p. 125.

Sniegowski, J.J. and Wolfer, W.G., 1984, "Proceedings of the Topical Conference on Ferritic Alloys for use in Nuclear Energy Technologies," J.W. Davis and D.J. Michel, Eds., (Warrendale, Pennsylvania: AIME).

Van Kampen, N.G., 1961, Can. J. Phys 39, 551.

Van Kampen, N.G., 1981, "Stochastic Processes in Physics and Chemistry," (Amsterdam: North-Holland) p. 214.

Wehner, M.F. and Wolfer, W.G., 1983a, Phys. Rev. A 27, 2663.

Wehner, M.F. and Wolfer, W.G., 1983b, Phys. Rev. A 28, 3003.

Wolfer, W.G. and Ashkin, M., 1975, J. Appl. Phys. 46, 547.

Wolfer, W.G. and Ashkin, M., 1976, J. Appl. Phys. 47, 791.

Wolfer, W.G. and Si-Ahmed, A., 1982, Phil. Mag. A 46, 723.

LIST OF CAPTIONS

Figure 1. The void bias factors vs. void radii for interstitials (solid line) and for vacancies (dashed lines) evaluated from Eqs. (18) and with the parameters listed in Table I.

Figure 2a. The transformed drift function vs. void radii obtained by neglecting the effect of the void size distribution at T = 873 K and a dose rate of 0.001 dpa/s.

Figure 2b. The transformed diffusion function vs. void radii obtained by neglecting the effect of the void size distribution at T = 873 K and a dose rate of 0.001 dpa/s.

Figure 3a. The void size distribution vs. void radii at various times obtained by neglecting the effect of the size distribution upon itself at T = 873 K and a dose rate of 0.001 dpa/s. Note the high concentration of unstable voids and the plateau-like size distribution of stable voids. The times indicated are in seconds.

Figure 3b. The void size distribution vs. void radii at various times obtained by considering the effect of the void size distribution itself on the microstructural parameters at T = 873 K and a dose rate of 0.001 dpa/s. Note the "pinching off" of the void size distribution at later times. This results in a lowering of the concentration of unstable voids as well as the isolation of a narrow size class of stable voids. The times indicated are in seconds.

Figure 4. The transformed drift function vs. void radii which led to the void size distributions of Fig. 3b evaluated at those times.

Figure 5. The potential function vs. void radii which led to the void size distributions of Fig. 3b evaluated at those times. Note how the nucleation barrier (the peak value of the potential) increases drastically with time.

Figure 6a. The void size distribution vs. void radii at various times with T = 673 K and a dose rate of 0.001 dpa/s.

Figure 6b. The void size distribution vs. void radii at various times with T = 673 K and a dose rate of 10^{-6} dpa/s.

Figure 7. Terminal void number densities vs. temperature at various dose rates. Solid circles - 10^{-6} dpa/s; open circles - 10^{-5} dpa/s; open squares - 10^{-4} dpa/s; solid squares - 10^{-3} dpa/s.

Figure 8. A comparison of the theoretical prediction of the terminal void number density vs. temperature with various neutron irradiation experiments.